Energy Equip. Sys. / Vol. 8/No. 3/Sep. 2020/ 277-296

ENERGY EQUIPSYS

Energy Equipment and Systems

http://energyequipsys.ut.ac.ir
www.energyequipsys.com

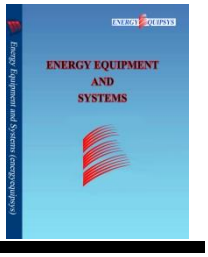

The use of waste heat recovery (WHR) options to produce electricity, heating, cooling, and freshwater for residential buildings

Authors

Ehsan Gholamian [a]
Pouria Ahmadi [a*]
Pedram Hanafizadeh [a]
Livio Mazzarella [b]

[a] School of Mechanical Engineering, College of Engineering, University of Tehran, P.O. Box 11155-4563, Tehran, Iran

[b] Department of Energy, Polytechnic University of Milan, Milan, Italy

Article history:

Received : 2 February 2020
Accepted : 25 June 2020

ABSTRACT

In recent years, there is a growing attention drawn to the area of building-integrated CCHP systems, due to its high capability in cost and energy saving. In this study, a residential scale multigenerational system is proposed to generate power by using solid oxide fuel cell and gas turbine (hybrid SOFC/GT), heating (by using HRSG), cooling (by using a double-effect absorption chiller) and freshwater (by using a Revers osmose plant). The system is modeled in engineering equation solver and studied from energy, exergy, economic and environmental standpoints. A parametric study is conducted in order to define the crucial decision variables in the system, and their effect on the overall exergy efficiency and unit product cost, along with the rate of freshwater production is observed. Results of the parametric study demonstrated that fuel utilization factor, stack temperature difference, current density, and the pressure ratio of air compressor have the most substantial influence on the behavior of the proposed system. Moreover, obtained results revealed that the energy and exergy efficiency of the system reaches 86.32% and 69.06%, respectively. In addition, the rate of freshwater production and unit product cost of the entire system becomes 256 L/day and 37.78 $/GJ.hr. Furthermore, the emission of the proposed system becomes 0.225 ton/MW.hr, which faces a 31% reduction compared to the standalone power generation system.

Keywords: Emission Reduction, Hybrid SOFC/GT, Residential-Scale CCHP, Freshwater.

1. Introduction

Rapid changes in population growth and the growing need to develop more power to this increasing population, has caused many fossil fuels depletion and lots of emission of GHG [1]. In this regard, the efficient use of energy sources has drawn more attention to itself as multigenerational systems [2]. Also, the total efficiency of thermal power plants in Iran is between 30-50% while considering 20% transmission losses; the distributed energy generation seems more perspective [3].

One of the best methods to utilize the energy efficiently is choosing the best prime mover to the multigenerational systems in residential applications [4,5] as many prime movers (PMs), is studied from the standpoint of energy and economical by the researchers.

High efficient combined cycles have been studied by many scientists in order to identify the better prime mover and find out whether or not the required power/heating/cooling capacity is met [6,7].

* Corresponding author: Pouria Ahmadi
School of Mechanical Engineering, College of Engineering, University of Tehran, P.O. Box 11155-4563, Tehran, Iran
Email: pahmadi@ut.ac.ir

The integration of an ORC with biomass fired Rankine cycle is studied by Behzadi et al. [8]. The obtained results indicate that the combination of the two systems causes a higher energetic and exergetic efficiency, which is 2.24% and 1.87%, respectively.

Moreover, to find out the better PM for an integrated energy system, Abbasi et al. [9] considered a CCHP system with GT and ICE. Their results point out that if both PMs are used as a hybrid system, in series mode, the energy efficiency and exergy efficiency will increase and become 87% and 62.8%, respectively. Also, they showed that operating costs in the optimum case would reduce up to 80%. Li et al. [10] studied an integrated CCHP system to find the optimal design and operating approach. Their study included the residential scale CCHP system and the systems which are suitable for hotels in china. They figured out that there is no economic gain in using CCHP systems for residential applications in china, however, for hotels, they demonstrate a crucial contribution to energy saving (42.28%), which is because of their comparatively unwavering electricity loads. Rajamand et al. [11] studied the miro-CHP system integrated with building in a load sharing method. Khademi et al. [12] studied the optimization of the combined cycle and found out that in an optimized case, the operation costs will decrease by 40%. Ghasemkhani et al. [13] optimized a solar-driven CCHP system. They found out that the maximum total cost rate, energy, and exergy efficiency are equal to 15.1 $/hr, 33%, and 36.47%, respectively. The technical performance of a multigenerational system based on solid oxide fuel cells for an educational building is investigated by Mehrpouya et al. [14]. The results showed that the efficiency of a single SOFC, The CHP system, and The CCHP system, reaches respectively, 45%, 58%, and 60%. Also, they comprehended that the capital recovery factor is 8.3 years for the whole system.

Investigation of a CCHP system based on GT Prime mover is carried out by Wang et al. [15]. The results in terms of fuel consumption demonstrated that combined system has 31% less fuel consumption than combined cycle. Furthermore, in another study, Li et al. [16] performed an analysis of a CCHP system and carried out the optimization based on energy loads coupling of residential and office buildings. The results showed that increased gas price will cause an increased air-conditioning cooling load. Besides, in another study, Jing et al. [17], used a SOFC as the primary prime mover of a CCHP system coupled with a residential building in China. Their study was comprised of a comparison between two CCHP systems, the prime movers of which was SOFC and ICE. Their results pointed out that SOFC based CCHP system shows significantly more efficiency and less GHG emission.

A methodology for sizing the prime movers of residential building integrated CCHP systems is introduced by Abbasi et al. [18]. In their study, the most relevant results were that determining the right CCHP system is a far better solution for all the environments in the study. Also CCCHP systems based on ICE proved to be beneficial in all case studies of the research.

Feng et al. studied the performance examination of a trigeneration case study with various cooling supply methods [19]. Another gas turbine-based CCHP system, along with a 4E analysis, is conducted by Moghimi et al. [20]. Their results showed that a 7% improvement in exergy efficiency and 12% in energy efficiency could be reached with the integration of the CCHP system instead of a standalone power generation system. Optimal management of a CCHP system based on SOFC, integrated with residential building applications, is studied by Al Moussavi et al. [21]. The two off-grid operation scenarios (following electrical load) and on-grid (following baseload) were studied. The optimized results showed that, from energy efficiency and cost, points of view, the CCHP system indicates excellent potential, as the maximum energy and exergy efficiency in optimized cases reaches 65.2% and 45.77%, and minimum cost rate reaches 22.22 cents/kWh.

Luo et al. [22]studied a multi supply multi demand control approach for combined cooling, heating, and power system primed with SOFC and gas turbine. Similarly, multi-

objective evaluation and optimization of a 5kW fuel cell integrated with the residential building are investigated by Chen et al. [23]. The optimized results disclosed that in optimal points, exergy efficiency, cost, and GHG emission are 39.9%, 29337.3 $, and gr, respectively. The proposal of an integrated energy system based on the SOFC system is carried out by Chitgar et al. [24]. The optimization results in their works showed that an optimal point exergy efficiency and total cost rate are 54% and 36.8 $/hr., respectively.

In this research article, a residential scale multigenerational system is introduced in order to supply the demands of a typical home, such as power (by employing SOFC/GT system), heating (by waste heat recovery using HRSG), cooling (by engaging Li/Br double-effect absorption chiller) and RO system to produce fresh water. A complete techno-economic survey is carried out to find the efficiencies and unit product cost of the system. To the best of author's knowledge, considering the literature survey, there is a little work done in the area of multigenerational systems in residential scale considering the following novelties:

- Comprehensive thermodynamic and analysis of the proposed system and defining the key decision variables.
- Defining detailed environmental analysis between different scenarios to reduce the GHG emission.
- Supplying the demands of the building as, power, heating, cooling, and freshwater.
- Conducting a parametric study and find inefficient components of the system to define possible candidates of component optimization.
- Using a Hybrid renewable energy system with considering heat recovery options for HRSG and refrigeration system along with producing freshwater.

Nomenclature

A	Area, m^2
c	Specific exergy cost, $/GJ
$\dot{C}$	Cost rate, $/h
$\dot{E}$	Exergy rate, kW
f	Exergoeconomic factor
F	Faraday constant, C/mol
$\Delta\bar{g}^0$	Change in molar Gibbs free energy, J/mol
h	Enthalpy, kJ/kmol
i_r	Interest rate
j	Current density, A/m^2
J	PEME current density, A/m^2
K	Equilibrium constant
LHV_f	Fuel lower heating value , kJ/kg
M	Molar mass, kg/mol
$\dot{m}_f$	Fuel mass flow rate
N	Operating hours, hr
$n_1,n_2,\ldots,n_7$	Mole number of reaction components
n_e	number of electrons produced per hydrogen mole
$\dot{n}$	Molar flow rate, mol/s
N_C	Number of cells in the stack
P	Pressure
PR	Pressure ratio
p_{H_2O}	The partial pressure of H_2O
p_{H_2}	The partial pressure of H_2
p_{O_2}	The partial pressure of O_2
Re	Reynolds number
RR	Recovery ratio
s	Specific entropy, kJ/kg.K
Sc	Schmidt number
R_{CR}	Cathode recycling ratio
$\bar{R}$	Universal gas constant, J/mol K
RO	Reverse Osmose
T	Temperature, K
T_g	Gasification temperature
U_f	Fuel utilization ratio
V	Voltage, V
V_0	Reversible potential, V
V_C	Cell voltage, V
V_{loss}	Loss voltage, V
V_N	Reversible cell voltage, V
w	Mole fraction of moisture in the biomass (kmol/kmol)
$\dot{W}$	Power, kW
y_i	Molar fraction
y_r	Extent of water gas shift reaction, mol/s
x_r	Extent of steam reforming reaction for methane, mol/s
$\dot{Z}$	cost rate of components, $/h
$\dot{Z}^{CI}$	Capital investment cost rate of components, $/h
$\dot{Z}^{OM}$	Operating and maintenance cost rate of components, $/h

Superscripts

ch	Chemical

ph	Physical

Subscripts and abbreviations

0	Dead state
act	Activation
AB	Afterburner
AC	Air Blower
an	Anode
AHX	Air heat exchanger
ca	Cathode
CEPI	Chemical Engineering Plant Cost Index
conc	Concentration
CRF	Capital recovery factor
D	Destruction
e	Electrolyte
FC	Fuel Blower
FHX	Fuel heat exchanger
i	Inlet
INV	DC to AC inverter
k	k^{th} component
L	Loss
GT	Gas turbine
CCHP	Combined cooling heating and power
CHP	Combined heating and power
PY	Present year
R	reforming
S	Shifting
SOFC	Solid oxide fuel cell
tot	Total

Greek letters

η_{pcy}	Polytrophic efficiency
$\eta_{mech,SE}$	Stirling mechanical efficiency
ε	Emission indicator
η_I	Energy efficiency
η_{II}	Exergy efficiency
φ	Maintenance factor
τ	Annual plant operation hours

2. System description and assumptions

Figure 1 demonstrates the schematics of the proposed residential-scale multigenerational energy system. The system is aimed to produce power, heating, and cooling along with freshwater for domestic applications. The system consists of 5 subsystems, the fuel cell and gas turbine or power production, the heat recovery steam generator for hot water production, the double-effect absorption chiller for cooling, and one reverse osmosis plant (RO) for freshwater production. The pressurized air and fuel are passed through air mixing and fuel mixing unit to the fuel cells cathode and anode respectively. The fuel cell generates electrical current and the high temperature products which contain, unburned fuels are put to the afterburner to increase the temperature of exhaust gases to further higher values. The high-temperature exhaust is then is passed through the gas turbine to generate power, which is used in the RO plant to produce fresh water. The gases which exit the gas turbine, are high enough to be able to be used to generate domestic hot water in HRSG (state 31 and 32). The final subsystem to produce cooling, is the double effect absorption chiller, the definition of which can be found in the literature [25]. The hot gases pass through the high-pressure generator of the absorption chiller and then is discharged to the environment. The main assumption and input values to render the analysis is gathered below as well as in Table 1.

- There is negligible heat loss from the components
- Steady-state conditions are applied
- Air and gas mixtures are modeled via ideal gas models
- Contact resistance in SOFC is neglected
- Kinetic and potential energy changes are small to consider
- Unburned gasses are fully oxidized at the exit of afterburner and combustion chambers

3. Modeling and analysis

The thermodynamic modeling of the proposed system is conducted in this section, with simultaneous solving of mass, energy, and exergy balance equations, considering each component as a single control volume. In order to carry out the exergoeconomic balance, the same procedure is applied to each component. The environmental impact assessment is carried out to find the emission reduction done by the proposed system.

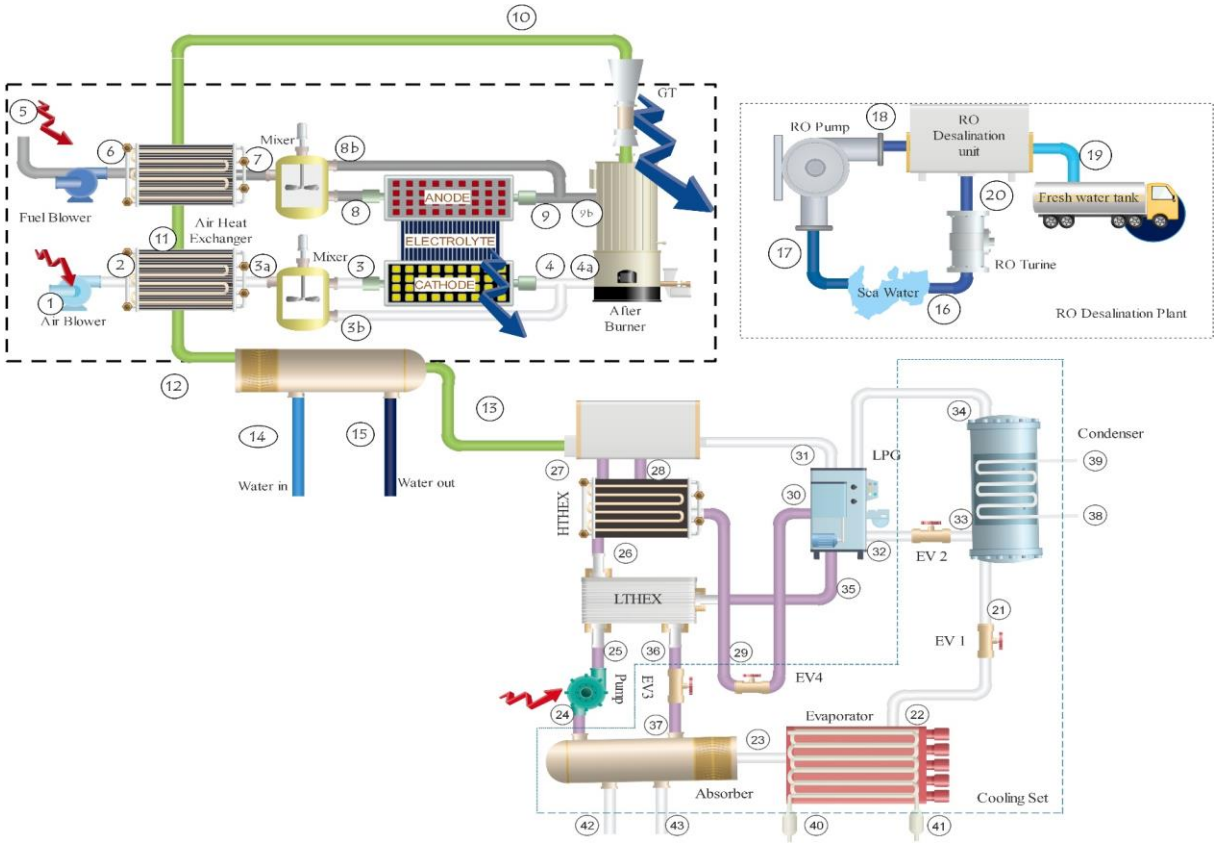

Fig. 1. Schematic diagram of the proposed multigenerational systems

Table 1. the input values to the multigenerational energy system [26,27]

Parameter	value	Parameter	value
SOFC system		**RO plant**	
j (A/m^2)	5000	b_n	7
U_f	0.85	$\eta_{RO\ pm}$ (%)	0.8
ΔT_{stack} (°C)	100	$\eta_{RO\ turbine}$ (%)	0.85
R_{AR}	0.4	K_m (m^{2}s/kgPa)	8.03×10^{-11}
R_{CR}	0.4	n	600
PR_{AC}	1.19	A_{mem}	40
PR_{FC}	1.19	R_c	0.9975
η_{inv}	0.97	d (mm)	0.71
A_a (m^2)	0.01	D_s (m^2/s)	$1.45\times107^{-}$
$T_{SOFC,inlet}$ (K)	1000	n_{pv}	42
j_{anode} (A/m^2)	6500	n_m	7
$j_{cathode}$ (A/m^2)	2500	C_k (\$)	1200
Effective diffusivity of gases - anode (cm^2/s)	0.2	C_{pv} (\$)	7000
Effective diffusivity of gases - cathode (cm^2/s)	0.05	RR	0.5
Anode thickness (mm)	0.5	**double-effect absorption chiller**	
Cathode thickness (mm)	0.05	T_{HPG} (°C)	130
Electrolyte thickness (mm)	0.01	T_{Abs} (°C)	35
Interconnect thickness (mm)	3	T_{Cond} (°C)	35
Cell numbers	11000	*Heat exchanger effectiveness*	0.7
Pressure drop through the stack (%)	2		
Pressure drop through the heat exchanger (%)	3		
Pressure drop through the afterburner (%)	5		
$\eta_{FC}=\eta_{AC}$	0.85		

3.1. Thermodynamic modeling

Mass, energy, and exergy balance equations are considered for each component as below [28,29]:

$$\sum \dot{m}_{in} = \sum \dot{m}_{out} \quad (1)$$

$$\dot{Q} - \dot{W} = \sum \dot{m}_{out}\, h_{out} - \sum \dot{m}_{in}\, h_{in} \quad (2)$$

$$\dot{E}_Q - \dot{E}_W = \sum \dot{m}_{out}\, e_{out} - \sum \dot{m}_{in}\, e_{in} + \dot{E}_D \quad (3)$$

In order to apply the equations above to the different subsystems, the following sections are introduced in detail:

3.1.1. SOFC system

The global reaction which happens in the SOFC system can be expressed as Eq. (4):

$$H_2 + \frac{1}{2}O_2 \rightarrow H_2O \quad (4)$$

In order to the supply the SOFC with a higher content of H2, the fuel, which is CH4, needs to be reformed. For this particular purpose, there are internal and external reformers [30]. The internal reformer is occupied in this research since it is cheaper.

At high temperature of the stack, the reforming and shifting equations occur at an equilibrium rate which is expressed as [26]:

$$lnK_R = -\frac{\Delta \bar{g}_R^0}{\bar{R}T_{FC,e}} = ln\left[\frac{(\dot{n}_{CO} + x_r - y_r) \times (\dot{n}_{H_2} + 3x_r + y_r - z_r)}{(\dot{n}_{CH_4} + x_r) \times (\dot{n}_{H_2O} - x_r - y_r + z_r)} \times \frac{P^2}{n_{tot,in}^2 + 2x_r}\right] \quad (5)$$

$$lnK_S = -\frac{\Delta \bar{g}_S^0}{\bar{R}T_{FC,e}} = ln\left[\frac{(\dot{n}_{CO_2} + y_r) \times (\dot{n}_{H_2} + 3x_r + y_r - z_r)}{(\dot{n}_{CO} + x_r - y_r) \times (\dot{n}_{H_2O} - x_r - y_r + z_r)}\right] \quad (6)$$

Additionally, in order to determine the amount of reacted H_2 as in equation four can be found employing Faraday's law:

$$j = \frac{n_e F z_r}{N_c A_c} \quad (7)$$

Wherein N_c, A_c, and n_e depict the Number of cells, area of cells, and the number of electrons shifted in the global reaction, respectively.

Besides, the fuel utilization factor is defined in order to find the amount of reacted hydrogen[31]:

$$U_f = \frac{z_r}{\dot{n}_{H_2} + 3x_r + y_r} \quad (8)$$

Energy balance of the SOFC is useful to find the situation o exiting streams from the stack and can be expressed as:

$$\dot{W}_{SOFC,stack,DC} = \dot{m}h_8 + \dot{m}h_4 - \dot{m}h_3 - \dot{m}h_7 \quad (9)$$

Moreover, the fuel cell output power is determined via electrochemical reaction and is as follows:

$$\dot{W}_{SOFC,stack,DC} = N_c A_c j V_c \quad (10)$$

$$\dot{W}_{SOFC,stack,AC} = \dot{W}_{SOFC,stack,DC} \times \eta_{inv} \quad (11)$$

In Eq. (10), j and V_c stand for the current density and cell voltage. The cell voltage is the difference between nominal voltage and loss voltages as:

$$V_c = V_N - V_{loss} \quad (12)$$

$$V_{loss} = V_{ohm} + V_{act} + V_{conc} \quad (13)$$

$$V_N = -\frac{\Delta G^0}{n_e F} - \frac{\bar{R}T_C}{n_e F} ln\left(\frac{p_{H_2O}}{p_{H_2}\sqrt{p_{O_2}}}\right) \quad (14)$$

In which V_{ohm} , V_{act}, V_{conc} is voltage loss, respectively corresponding to ohmic overpotential, activation overpotential, and concentration overpotential [32,33].

3.1.1 Reverse osmose system

In a standard RO system which consists of a pump, turbine and heat exchanger, the input power can be expressed in terms of RO hydro turbine power ($\dot{W}_{turbine}$) and Pump power($\dot{W}_{pump}$) as [34,35]:

$$\dot{W}_{net} = b_n(\dot{W}_{pm} - \dot{W}_{turbine}) \quad (15)$$

In which b_n is several trains, and its value is 7 in this research. Also, the power of the turbine and pump is as expressed in the following [27]:

$$\dot{W}_{Pump} = \frac{\Delta P \dot{m}_{20}}{\rho_{20}\eta_{pm}} \quad (16)$$

$$\dot{W}_{turbine} = \frac{\Delta P \dot{m}_{20}\eta_{turbine}}{\rho_{20}} \quad (17)$$

Here, ΔP, η_{pm}, and $\eta_{turbine}$ are transmembrane pressure, RO pump, and hydro-turbine isentropic efficiencies, respectively. The rate of the objective freshwater mass flow rate ($\dot{m}_{44}$) is related to the brine mass flow rate ($\dot{m}_{43}$) and the recovery ratio (RR) as one of the practical representative of the membrane. Further discussion about the reverse osmose plant can be found in the literature [27,34].

Energy and exergy balance equations for SOFC and other components like heat exchangers, compressors, pumps, and turbine, as well as expansion valves, are tabulated in Table 2 based on Eqs. (1-3).

3.3. Exergoeconomic analysis

In order to demonstrate the effectiveness of the system, the economic analysis of every energy system is vital. There are different methods in the literature to carry out the economic factors of the system, among which (SPECO), specific costing theory is used effusively to conduct the financial aspects of energy systems.

In this approach, the component's exergy cost is calculated by writing exergy balance equations and solving them with cost balances concurrently. Cost balances are

Table 2. Energy and Exergy rate balances for the system components in different scenarios [36]

Component	Energy balance	Exergy balance
	SOFC	
SOFC	$\dot{W}_{SOFC,stack,DC} = \dot{m}h_8 + \dot{m}h_3 - \dot{m}h_4 - \dot{m}h_9$	$\dot{E}_{D,SOFC}=\dot{E}_8+\dot{E}_3-(\dot{E}_4+\dot{E}_9)-\dot{W}_{SOFC,stack,DC}$
AHX	$0 = \dot{m}h_{11} + \dot{m}h_2 - \dot{m}h_{3a} - \dot{m}h_{12}$	$\dot{E}_{D,AHX}=\dot{E}_{11}-\dot{E}_{12}-(\dot{E}_{3a}-\dot{E}_2)$
Fuel Blower	$\dot{W}_{F.B} = \dot{m}h_6 - \dot{m}h_5$	$\dot{E}_{D,FC}=\dot{W}_{FC}-(\dot{E}_6-\dot{E}_5)$
Air Blower	$\dot{W}_{A.B} = \dot{m}h_2 - \dot{m}h_1$	$\dot{E}_{D,AC}= \dot{W}_{AC}-(\dot{E}_2-\dot{E}_1)$
Afterburner	$0 = \dot{m}h_{9b} + \dot{m}h_{4a} - \dot{m}h_{10}$	$\dot{E}_{D,AB}=\dot{E}_{4a}+\dot{E}_{9b}-\dot{E}_{10}$
Anode mixer	$0 = \dot{m}h_7 - \dot{m}h_{8b} - \dot{m}h_8$	$\dot{E}_{D,AM}= \dot{E}_7+\dot{E}_{8b}-\dot{E}_8$
Cathode mixer	$0 = \dot{m}h_{3a} - \dot{m}h_3 - \dot{m}h_{3b}$	$\dot{E}_{D,CM}= \dot{E}_{3b}+\dot{E}_{3a}-\dot{E}_3$
	MGT	
GT	$\dot{W}_{GT} = \dot{m}h_{10} - \dot{m}h_{10a}$	$\dot{E}_{D,T} = \dot{E}_{10a} - \dot{E}_{10} - \dot{W}_T$
	Li/Br double effect absorption chiller	
HPG	$\dot{Q}_{HPG} = \dot{m}_{31}h_{31} + \dot{m}_{28}h_{28} - \dot{m}_{327}h_{27}$	$\dot{E}_{D,HPG} = \dot{E}_{13} + \dot{E}_{27} - \dot{E}_{31} - \dot{E}_{28} - \dot{E}_{st.}$
LPG	$\dot{m}_{31}h_{31} + \dot{m}_{30}h_{30} - \dot{m}_{34}h_{34} - \dot{m}_{35}h_{35} - \dot{m}_{35}h_{35}=0$; $\dot{Q}_{LPG} = \dot{m}_{31}h_{31} - \dot{m}_{34}h_{34}$	$\dot{E}_{D,LPG} = \dot{E}_{31} + \dot{E}_{30} - \dot{E}_{32} - \dot{E}_{34} - \dot{E}_{35}$
Evap.	$\dot{Q}_{evap} = \dot{m}_{22}h_{22} - \dot{m}_{23}h_{23}$	$\dot{E}_{D,evap} = \dot{E}_{22} + \dot{E}_{40} - \dot{E}_{28} - \dot{E}_{41}$
Cond.	$\dot{Q}_{cond} = \dot{m}_{14}h_{14} + \dot{m}_{13}h_{13} - \dot{m}_{26}h_{26}$	$\dot{E}_{D,Cond} = \dot{E}_{14} + \dot{E}_{13} + \dot{E}_{20} - \dot{E}_{21} - \dot{E}_{26}$
Abs.	$\dot{Q}_{abs} = \dot{m}_{23}h_{23} + \dot{m}_{24}h_{24} - \dot{m}_{37}h_{37}$	$\dot{E}_{D,Abs} = \dot{E}_{42} + \dot{E}_{24} + \dot{E}_{23} - \dot{E}_{37} - \dot{E}_{43}$
Pump	$h_{25} = h_{24} + \frac{\dot{W}_p}{\dot{m}_{24}}, \dot{W}_p = \dot{m}_{24} \times (P_{HPG} - P_{abs})/\eta_p \times \rho_{24}$	$\dot{E}_{D,P} = \dot{E}_{24} - \dot{E}_{25} + \dot{W}_p$
LTHEX	$h_{26} = h_{25} - (h_{25} - h'_{26}) \times \eta_{LTHEX}$ $h_{26} = \frac{\dot{m}_{25}}{\dot{m}_{26}}(h_{25} - h_{26}) + h_{15}, h'_{26} = h(T_{abs}, x_{25})$	$\dot{E}_{D,LTHEX} = \dot{E}_{25} + \dot{E}_{35} - \dot{E}_{26} - \dot{E}_{36}$
HTHEX	$h_{29} = h_{28} - (h_{28} - h'_{29}) \times \eta_{HTHEX}$ $h_{27} = \frac{\dot{m}_{28}}{\dot{m}_{26}}(h_{28} - h_{29}) + h_{26}, h'_{29} = h(T_{26}, x_{28})$	$\dot{E}_{D,HTHEX} = \dot{E}_{26} + \dot{E}_{28} - \dot{E}_{27} - \dot{E}_{29}$
E.V	$h_i = h_e$	$\dot{E}_{D,HTR} = \dot{E}_i - \dot{E}_e$
	RO system	
RO pump	$\dot{W}_{Pump} = \frac{\Delta P \dot{m}_{17}}{\rho_{17}\eta_{pm}}$	$\dot{E}_{D,RO,Pm} = \dot{W}_{RO,Pm} - (\dot{E}_{17} - \dot{E}_{418})$
RO desalination unit	$\dot{W}_{net} = b_n(\dot{W}_{pm} - \dot{W}_{turbine})$	$\dot{E}_{D,RO} = (\dot{E}_{19} - \dot{E}_{20}) - \dot{E}_{19}$
RO turbine	$\dot{W}_{turbine} = \frac{\Delta P \dot{m}_{20}\eta_{turbine}}{\rho_{20}}$	$\dot{E}_{D,RO,Turbine} = (\dot{E}_{20} - \dot{E}_{16}) - \dot{W}_{RO,Turbine}$

considered for each system component as a single control volume, to find the exergy cost of each stream as below [37]:

$$\sum \dot{C}_{out,k} + \dot{C}_{w,k} = \sum \dot{C}_{in,k} + \dot{C}_{q,k} + \dot{Z}_k \quad (26)$$

$$\dot{Z}_k = \dot{Z}_k^{CI} + \dot{Z}_k^{OM} \quad (27)$$

$$\dot{C} = c\dot{E} \quad (28)$$

$$\dot{C}_{out} = c_{out}\dot{E}_{out} \quad (29)$$

$$\dot{C}_q = c_q\dot{E}_q \quad (30)$$

$$\dot{C}_w = c_w\dot{E}_w \quad (31)$$

where *c*, $\dot{Z}_k^{OM}$ and $\dot{C}$ respectively represents the specific exergy cost, price of operation and maintenance, and the cost rate in each element. Moreover, yearly Levelized capital investment is delimited as below for each component [38]:

$$\dot{Z}_k^{CI} = \left(\frac{CRF}{\tau}\right) Z_k \quad (32)$$

where τ is the total operation time of the energy system in one year, which is assumed 8760 hr in this research and *CRF* is the capital recovery factor that can be defined as [39]:

$$CRF = \frac{i_r(1+i_r)^n}{(1+i_r)^n - 1} \quad (33)$$

The Z_k for the present year (2020) is estimated by using the equations of cost at the base year, which gathered in Table 2 [40]:

$$Cost\ at\ present\ year = Original\ cost \times \frac{CEPCI\ of\ the\ present\ year}{CEPCI\ of\ the\ base\ year} \quad (34)$$

In which the number of plant operation hour and rate of interest is respectively demonstrated by n and i_r. Table 3 represents the Purchased cost equations for different elements in the proposed multigenerational system.

Table 3: Purchased cost equations for different elements in the proposed multigenerational system [41–43]

Component	Cost equation
	SOFC
SOFC	$Z_{SOFC} = A_a N_{FC}(2.96T_{FC,e} - 1907)$
AHX	$Z_{AHX} = 3 \times \left[130 \times \left(\frac{A_{AHX}}{0.093}\right)^{0.78}\right]$
Fuel and Air Blowers	$Z_{AC} = Z_{AF} = 91562 \times \left(\frac{\dot{W}_{AC}}{455}\right)^{0.67}$
Afterburner	$Z_{AB} = \frac{46.08 \times \dot{m}_4}{(0.955 - (P_{11}/P_4))}(1 + e^{0.018T_{11} - 26.4})$
Inverter	$Z_{inv} = 10^5 \times \left(\frac{\dot{W}_{SOFC,DC}}{500}\right)^{0.7}$
GT	$Z_{GT} = (\frac{479.34\dot{m}_g}{0.92 - \eta_{st}})\ (Ln\left(P_{inlet}/P_{outlet}\right))(1 + e^{0.036T_{inlet} - 54.4})$
	Li/Br double effect absorption chiller
HPG	$Z_{HPG} = 17500(\frac{A_{HPG}}{100})^{0.6}$
LPG	$Z_{LPG} = 17500(\frac{A_{LPG}}{100})^{0.6}$
Evap.	$Z_{Evap} = 16000(\frac{A_{Evap}}{100})^{0.6}$
Cond.	$Z_{Cond} = 8000(\frac{A_{Cond}}{100})^{0.6}$
Abs.	$Z_{ABS} = 16000(\frac{A_{ABS}}{100})^{0.6}$
Pump	$Z_{Pm} = c_1 \dot{W}_{Pm}^{0.65}$ c_1=1000 \$/kW$^{0.65}$
LTHEX	$Z_{HTHEX} = 12000(\frac{A_{HTHEX}}{100})^{0.6}$
HTHEX	$Z_{LTHEX} = 12000(\frac{A_{LTHEX}}{100})^{0.6}$
	RO unit
RO unit	Z_{RO}=0.98×$\dot{m}_{44}^3$
	i_r=0.12, *n*=20 years

$c_{F,k}$, $c_{P,k}$, $\dot{C}_{D,k}$, $\dot{C}_{L,k}$, and f_k are depicted as below in order to apprehend the performance of the system from exergoeconomic point of view [44]:

$$c_{F,k} = \frac{\dot{C}_{F,k}}{\dot{E}_{F,k}} \quad (35)$$

$$c_{P,k} = \frac{\dot{C}_{P,k}}{\dot{E}_{P,k}} \quad (36)$$

$$\dot{C}_{D,k} = c_{F,k}\dot{E}_{D,k} \quad (37)$$

$$f_k = \frac{\dot{Z}_k}{\dot{Z}_k + \dot{C}_{D,k+}\dot{C}_{L,k}} \quad (38)$$

$$r_k = \frac{c_{P,k} - c_{F,k}}{c_{F,k}} \quad (39)$$

The terms in Eqs. (35-39) are the unit cost of fuel, the unit cost of the product, the cost rate of exergy destruction, the cost rate of exergy loss, and the exergoeconomic factor, respectively. Furthermore, in order to give a better insight into the capital and operating and maintenance costs against exergy inefficiency costs, the exergoeconomic factor is given as Eq. (38).

The auxiliary equations and cost balance equations, which is necessary to solidify the economic analysis are tabulated in Table 4

3.4 Performance Evaluation

The evaluation of the performance of the multigenerational system is observed by considering the exergy efficiency and unit product cost of the system as defined by Eqs. 40 and 41 below [45–47]:

$$\eta_{II} = \frac{\dot{W}_{net} + \dot{E}_{heating} + \dot{E}_{cooling} + \dot{E}_{19}}{\dot{E}_F} \quad (40)$$

where input chemical exergy of fuel is presented by $\dot{E}_F$ [28]. And $\dot{E}_{heating} = \dot{E}_{15} - \dot{E}_{14}$ also cooling and heating systems exergy is defined as: $\dot{E}_{cooling} = \dot{E}_{41} - \dot{E}_{42}$ and $\dot{E}_{44}$ denotes the chemical exergy of produced freshwater.

Table 4: Auxiliary equations and cost balances for different elements in the proposed multigenerational system

Component	Energy balance	Exergy balance
	SOFC	
SOFC	$\dot{C}_3+\dot{C}_8+\dot{Z}_{SOFC,stack,PY}=\dot{C}_4+\dot{C}_9+\dot{C}_{W,SOFC,stack}$	$c_4=c_{W,SOFC,DC}$ $c_9=c_{W,SOFC,DC}$
AHX	$\dot{C}_2+\dot{C}_{11}+\dot{Z}_{AHX,PY}=\dot{C}_{12}+\dot{C}_{3a}$	$c_{11}= c_{12}$
Fuel Blower	$\dot{C}_{W,FC}+\dot{C}_5+\dot{Z}_{FC,PY}=\dot{C}_6$	$c_{W,FC}=c_{W,SOFC,AC}$
Air Blower	$\dot{C}_{W,AC}+\dot{C}_1+\dot{Z}_{AC,PY}=\dot{C}_2$	$c_1=0$ $c_{W,AC}=c_{W,SOFC,AC}$
Afterburner	$\dot{C}_{9b}+\dot{C}_{4a}+\dot{Z}_{AB,PY}=\dot{C}_{10a}$	$C_{9b}= c_{8b}$, $c_{4a}= c_{3b}$ $c_{9b}= c_9$, $c_{3b}= c_4$
Anode mixer	$\dot{C}_8+\dot{C}_{8b}+\dot{Z}_{AM,PY}(0)=\dot{C}_8$	N/A
Cathode mixer	$\dot{C}_{3b}+\dot{C}_{3a}+\dot{Z}_{CM,PY}(0)=\dot{C}_3$	N/A
Inverter	$\dot{C}_{W,SOFC,DC}+\dot{Z}_{I,PY}=\dot{C}_{W,SOFC,AC}$	N/A
GT	$\dot{C}_{10a} + \dot{Z}_{GT} = \dot{C}_{10} + \dot{C}_{47}$	$C_{10} = c_{10a}$
	Li/Br double effect absorption chiller	
HPG	$\dot{C}_{27}+ \dot{C}_{QEx} +\dot{Z}_{HPG}=\dot{C}_{28}+ \dot{C}_{31}$	$\frac{\dot{C}_{21}}{\dot{m}_{21}(e_{21}-e_{28})} = \frac{\dot{C}_{27}(e_{28}-e_{31})}{\dot{m}_{27}(e_{21}-e_{27})(e_{28}-e_{27})} + \frac{\dot{C}_{28}}{\dot{m}_{28}(e_{28}-e_{27})}$
LPG	$\dot{C}_{31}+ \dot{C}_{30} +\dot{Z}_{LPG}=\dot{C}_{34}+ \dot{C}_{35}+ \dot{C}_{32}$	$\frac{\dot{C}_{24}}{\dot{m}_{24}(e_{24}-e_{30})} = \frac{\dot{C}_{30}(e_{35}-e_{34})}{\dot{m}_{30}(e_{24}-e_{20})(e_{25}-e_{20})} + \frac{\dot{C}_{35}}{\dot{m}_{25}(e_{25}-e_{30})}$
Cooling Set	$\dot{C}_{34}+ \dot{C}_{33} +\dot{Z}_{COND}=\dot{C}_{21}+ \Delta\dot{C}_{COND}$ $\dot{C}_{33}+ \dot{C}_{37} +\dot{Z}_{ABS}=\dot{C}_{23}+ \Delta\dot{C}_{ABS}$ $\dot{C}_{32}+ \dot{C}_{34} + \dot{C}_{29} + \dot{C}_{37}$ $+\dot{Z}_{ABS}+\dot{Z}_{COND}+\dot{Z}_{EVAP}+3\dot{Z}_{E.V} =$ $\Delta\dot{C}_{COND}+\Delta\dot{C}_{ABS}+\dot{C}_{33}-\dot{C}_{32}+\dot{C}_{24}+\dot{C}_{30}$	$\frac{\dot{C}_{23}+\dot{C}_{24}}{\dot{E}_{23}+\dot{E}_{24}} = \frac{\dot{C}_{11}}{\dot{E}_{11}}$ $\frac{\dot{C}_{23}+\dot{C}_{27}}{\dot{E}_{23}+\dot{E}_{27}} = \frac{\dot{C}_{24}}{\dot{E}_{24}}$ $c_{21}= c_{22}$, $c_{32}= c_{33}$, $c_{29}= c_{30}$ $c_{22}= c_{23}$, $c_{26}= c_{27}$, $c_{32}= c_{33}$
Pump	$\dot{C}_{24} + \dot{Z}_{Pm}= \dot{C}_{25}$	$c_{24}= c_{25}$
LTHEX	$\dot{C}_{25}+ \dot{C}_{35} +\dot{Z}_{HTHEX}=\dot{C}_{36}+ \dot{C}_{26}$	$c_{26}= c_{36}$
HTHEX	$\dot{C}_{26}+\dot{C}_{28} +\dot{Z}_{LTHEX}= \dot{C}_{27}+\dot{C}_{29}$	$c_{28}= c_{29}$
	Ro unit	
RO	$\dot{C}_{43}+\dot{Z}_{RO,PY}=\dot{C}_{44}+\dot{C}_{45}$	N/A

By writing overall cost balance to the system, considering the while the multigenerational system as a control volume, the total unit product cost can be expressed as[48]:

$$c_{p,tot} = \frac{\sum_{i=1}^{n_k} \dot{Z}_k + \sum_{i=1}^{n_F} \dot{C}_{F_i}}{\sum_{i=1}^{k} \dot{E}_{P_i}} \quad (41)$$

c_F is the price of input fuel in Iran and is considered to be 0.04 cent/m^3 in Iran.

Also in order to evaluate the heating and power capacity of the system, the produced heating and power is given by Eqs. 42 and 43:

$$\dot{W}_{net} = \dot{W}_{SOFC} - \dot{W}_{Compressors} - \dot{W}_{Pump} \quad (42)$$

$$\dot{Q}_{heating} = \dot{h}_{15} - \dot{h}_{14} \quad (43)$$

3.5 Environmental impact assessment

Reduced GHG emission and environmental sustainability are one of the outcomes of efficient use and integration of energy systems. In this regard, the researchers have developed a sustainability index in the literature [49,50], in which emitted CO_2 is of pronounced importance.

The CO2 emission for different cases in the proposed system is considered, b integrating the step by step a single generation. The index shows great potential and motivation of the multigenerational systems by considering the following subsystems: 1) power generation with a hybrid system of SOFC/GT is found, and the exhaust gases are discharged to the atmosphere 2) hybrid SOFC/GT as well as HRSG is considered 3) The multigenerational system based on prime mover and HRSG along with absorption chiller and Ro unit is used.

$$\varepsilon_{em,1} = \frac{\dot{m}_{CO_2,emitted}}{\dot{W}_{net}} \quad (44)$$

$$\varepsilon_{em,2} = \frac{\dot{m}_{CO_2,emitted}}{\dot{W}_{net} + \dot{Q}_{heating}} \quad (45)$$

$$\varepsilon_{em,3} = \frac{\dot{m}_{CO_2,emitted}}{\dot{W}_{net} + \dot{Q}_{heating} + \dot{Q}_{cooling} + \dot{m}_{H2O} HHV} \quad (46)$$

4. Results and discussion

In this section, the results of the parametric study to define the key effective variables on the system performance are carried out. Also, the exergy and exergoeconomic results are pointed out in order to show the system's cost-efficiency. Finally, the results of the environmental impact are shown to represent the motivation of the multigenerational system in the reduction of GHG emission.

4.1 Verification of developed models

In order to be certain of the accuracy of the modeling and, therefore, the precision of results, the validation and verification of different subsystems in the proposed energy system is presented here.

The accuracy of the modeling for the: 1) SOFC system validated using the data reported by Tao et al. [51], 2) RO system verified using the data published by Nemati et al. [52], and 3) double-effect absorption chiller verified using the results reported by Gomri and Hakimi is used [53], Are presented respectively in Figure 2, Table 5 and Table 6.

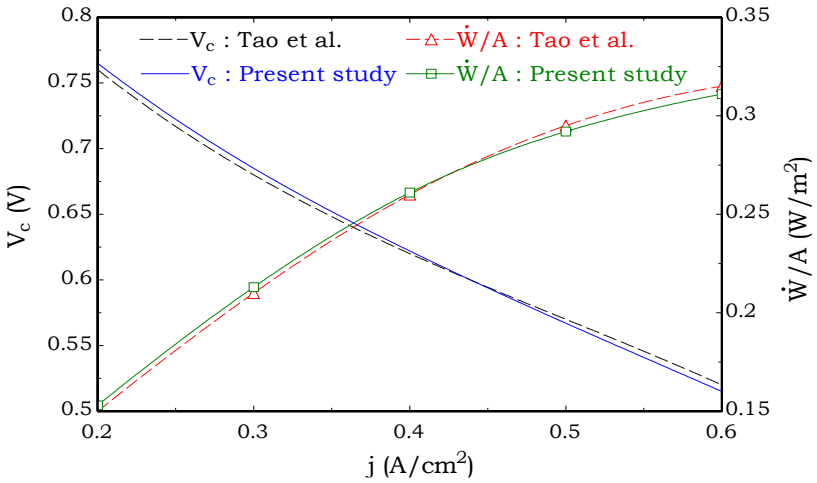

Fig.2. Comparison of the results for SOFC modeling with the results presented by Tao et al [51]

Table 5. Comparison of the results for RO modeling with the results presented by Nemati et al. [52].

Variable	Present model	Nemati *et al.* [52]
RO pump power consumption (kW)	1143	1185
Feed water volume flow rate (m^3/h)	485.7	485.9
Salt rejection percentage (%)	0.9944	0.9944
Rejected water salt concentration (g/kg)	64.13	64.16
Fresh water salt concentration (g/kg)	0.248	0.252
Transmembrane pressure (kPa)	6850	6843

Table 6. Comparison of the results for double effect chiller modeling with the results presented by Gomri and hakimi [53]

Constituent	Symbol	Present work (kW)	Experiment (kW) [53]
HP generator	Q_g	252.5	252.407
Condenser	Q_{cd}	167.3	167.205
Evaporator	Q_{ev}	300	300
Absorber	Q_{ab}	385.3	385.236
Pump	W	0.054	0
	COP	1.188	1.189

4.2. Parametric study results

The effect of system design parameters on the performance of the system is studied in this section. Figure 3 shows the impact of stack temperature difference on exergy efficiency and unit product cost, along with net power output and heating capacity. According to Fig.3, when the stack temperature difference is increased from 80 oC to 150 oC, unit product cost reduces from 40.43 (S/GJ) to 34.38 (S/GJ). Also, exergy efficiency reaches a maximum of 69.07%, corresponding to 102 oC temperature difference. This is mainly because increasing stack temperature difference causes a reduction in power and an increase in heating capacity from 38.5 kW to 148 kW.

Fuel utilization factor is far most believed to be one of the crucial parameters which affect the system performance, the effect of which is shown in Fig.4. If the fuel utilization factor is increased, the maximum exergy efficiency of 69.2% is reached at the corresponding value of 0.83. Also, a minimum of 23.6 ($/GJ) can be achieved for the unit product cost. This is, however, in case the net power output and heating capacity are both decreased when the fuel utilization factor is increased.

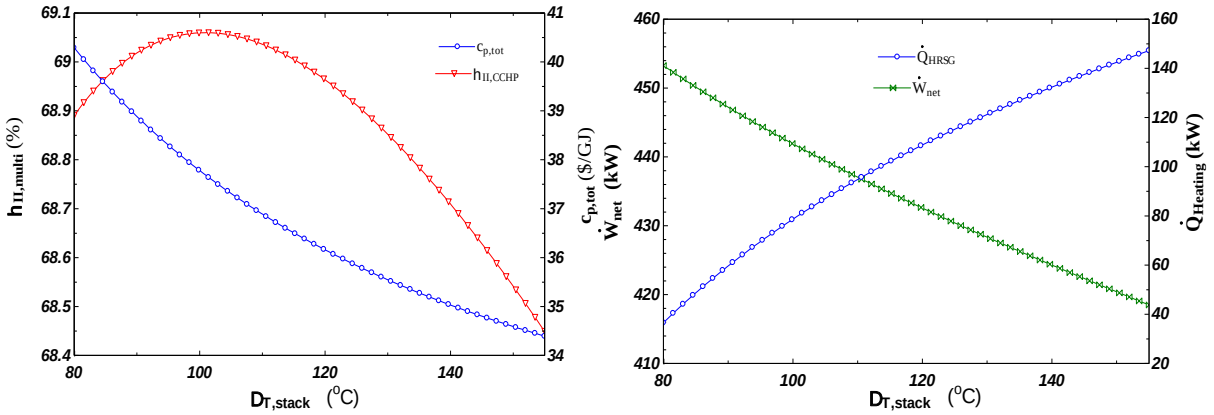

Fig.1. Effect of stack temperature difference on exergy efficiency and unit product cost along with net power output and heating capacity

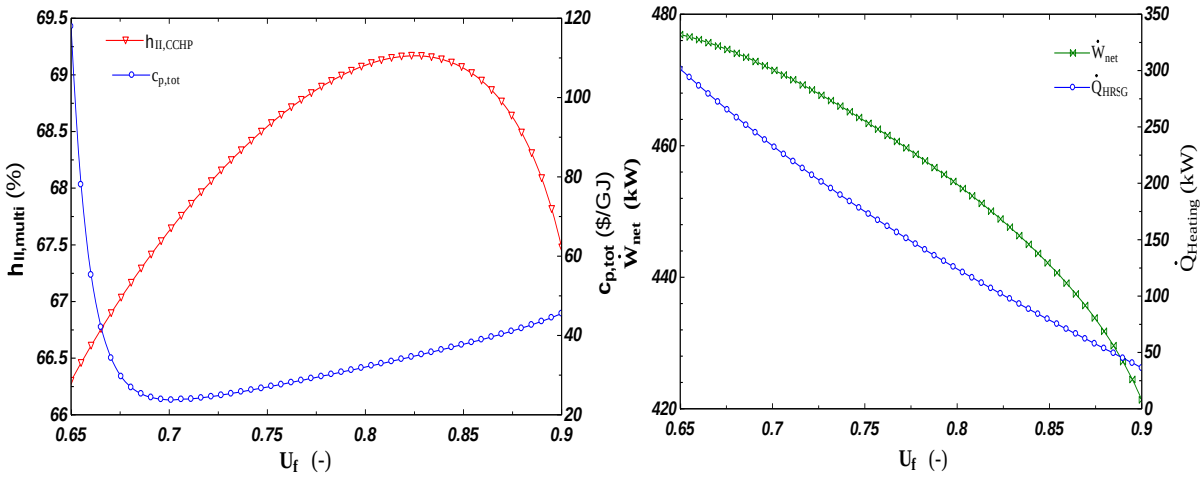

Fig.2. Effect of fuel utilization factor on exergy efficiency and unit product cost along with net power output and heating capacity

The impact of the current density of SOFC on exergy efficiency and unit product cost along with net power output and heating capacity is signposted in Figure 8. According to this figure, increasing current density from 2500 (A/m^2) to 6100 (A/m^2) causes an increase in both heating capacity and produced power. However, the unit product cost decreases from the rise in power production rate from 55.08 ($/GJ) to 35.01 ($/GJ).

The last but not the least important parameter to be studied here is the pressure ratio of air and fuel compressors, which is depicted in Figure 6. According to this figure, when increasing pressure ratio from 1.1 to 2.1 reduces the power output, according to the higher power needed to run the compressors, also it causes an increase in the heating capacity from 72 kW to 126 kW. These changes affect the unit product cost and exergetic efficiency in a manner that exergy efficiency is decreased, and unit product cost is increased by 2.74% and 26.1%, respectively.

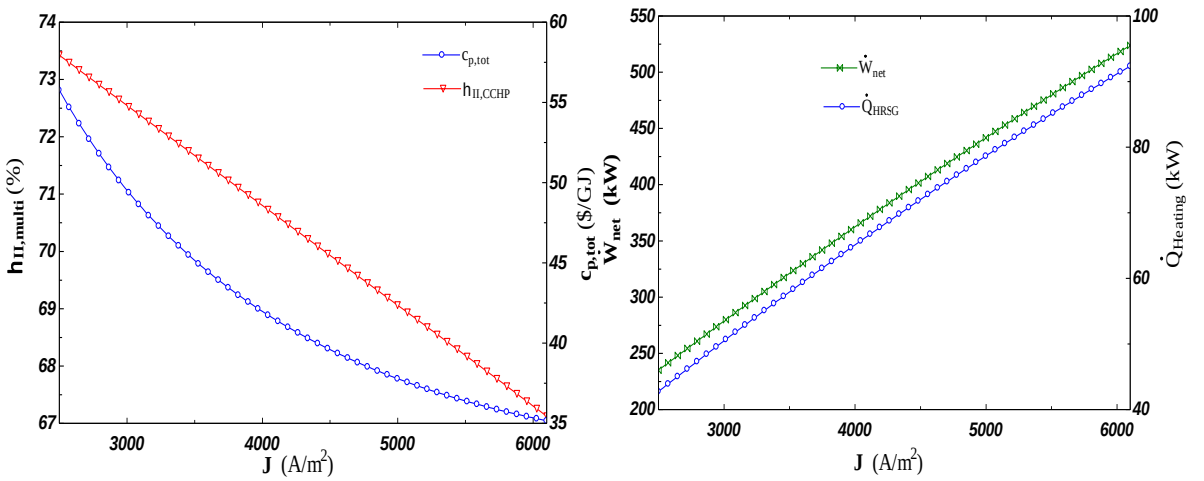

Fig.3. Effect of current density on exergy efficiency and unit product cost along with net power output and heating capacity

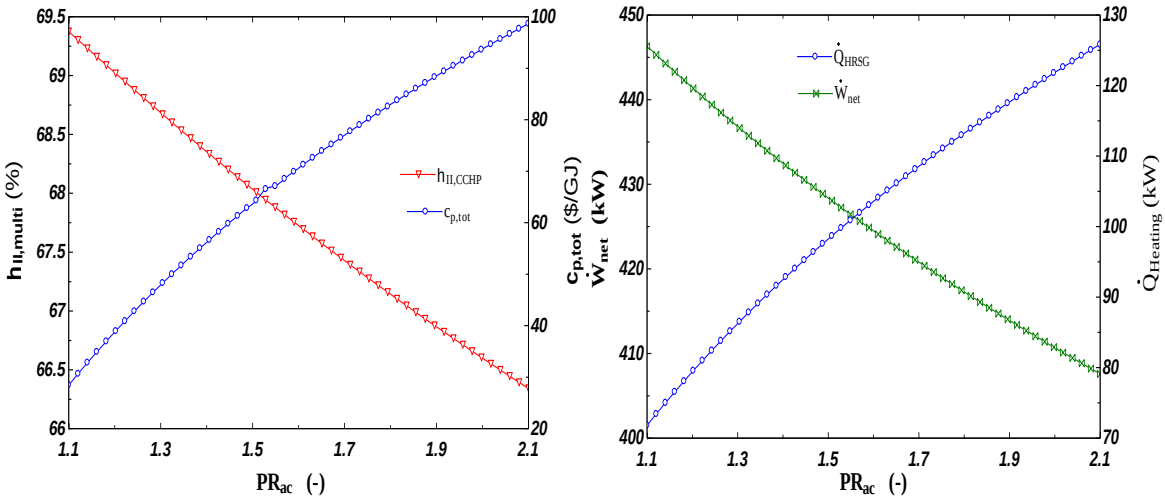

Fig.4. Effect of air compressor pressure ratio on exergy efficiency and unit product cost along with net power output and heating capacity

Another essential factor of the proposed multigenerational system is the amount of produced freshwater in one day. Figures 7 and 8 illustrate the effect of critical variables in the rate of change in freshwater production. According to figure 7, which shows the impact of the temperature difference and fuel utilization factor on the rate of the freshwater output, increasing the fuel utilization factor has a positive impact on the freshwater production rate; however, the decrease of stack temperature difference is favorable for this purpose. The increase of stack temperature difference from 80 to 150 will result in a 25.33% decrease in the rate of freshwater production.

Figure 8 shows the effect of increasing pressure ratio of air compressor and current density on the rate of freshwater production. It is evident that increasing current density has a positive effect on the freshwater production rate as it experiences 24.9% increase while increasing current density from 2500(A/m2) to 6100 The vital aspect of this figure, however, is that with increasing fuel compressor pressure ratio, the rate of fresh water reaches a minimum at 1.41 which is equal to 255.4 kg/day.

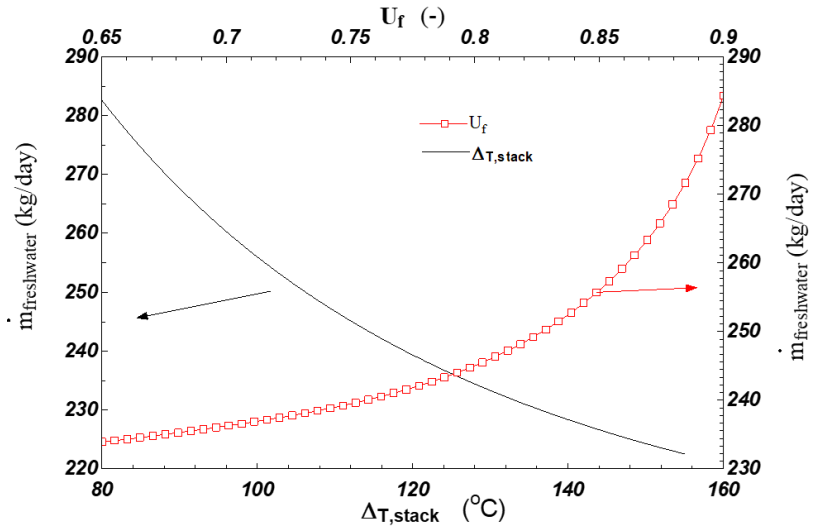

Fig. 5. Effect of stack temperature difference and fuel utilization factor on fresh water production

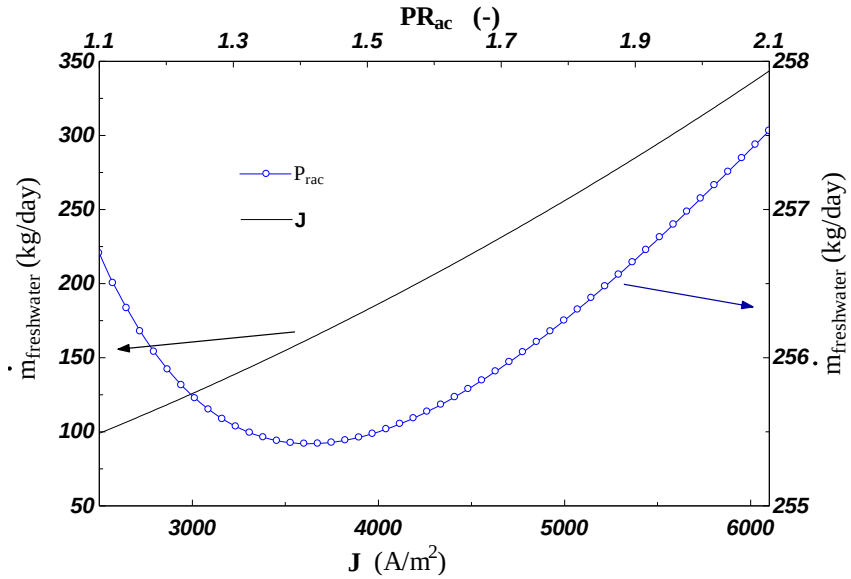

Fig. 6. Effect of current density and pressure ratio of air compressor on fresh water production

4.3. Exergy and exergoeconomic results

In order to see the performance of the multigenerational system from exergy and economic point of views, the exergoeconomic factors such as cost of fuel, and cost of product along with destructed cost and lost cost along with exergy indicators as exergy destruction, the exergy of fuel, exergy of product, and lost exergy is presented in Table 7.

According to Table 7, Air heat exchanger, SOFC, and afterburner with exergy destruction of respectively 120kW, 52.16kW, and 42.62 kW has the highest exergy destruction rates among the other components. This is because three significant irreversibility sources such as chemical reaction, mixing, temperature difference exist in these components more than others.

The table also shows exergoeconomic factors and the cost of each component, among which the last column of the table is worth-discussing. The exergoeconomic factor (f), as in equation 38, is defined as the cost of the components divided by the cost of exergy destruction and lost cost from the component. A high value of this factor indicates that a decrease shall be made in the capital investment of this component at the expense of its exergetic efficiency. On the other hand, a low value of this factor calculated for a significant component suggests that cost saving in the entire system might be achieved by improving the component efficiency (reducing exergy destruction) even if the capital investment for the component will increase. Examples of this case are fuel heat exchanger and air heat exchanger with 2.92% and 10.26% exergoeconomic factors.

Furthermore, the Sankey diagram of the proposed system is depicted in Figure 9 in order to illustrate the exergy flows of the proposed system. The width of each arrow is proportional to the amount of exergy flow in the stream. This figure helps in understanding the flow of the proposed system effectively.

4.4. Results of environmental impact assessment

Figure 10 illustrates the overall performance indicators of the proposed energy system. According to this figure, three different scenarios are studied, which is power generation system (with energy and exergy efficiency of 66.67% and 64.73 % respectively and GHG emission of 0.29 ton/MW.hr), the CHP system (with energy and exergy efficiency of 78.54% and 68.65 % respectively and GHG emission of 0.228 ton/MW.hr), and multigenerational system (with energy and exergy efficiency of 86.32% and 69.06 % respectively and GHG emission of 0.225 ton/MW.hr). This figure shows great importance and motivation for using the

CCHP system since it causes a significant increase in efficiency and a significant reduction in GHG emission (31%). Also, another important aspect of this figure is that the second law of thermodynamics pays attention to the quality of the energy streams and not the quality, this is the reason why the exergy efficiency is not as much increasing as energy efficiency in CCHP system compared to standalone power generation system.

Table 7. Exergy and exergoeconomic parameters of components in the proposed multigenerational energy system

	$\dot{E}_D$ (kW)	$\dot{E}_F$ (kW)	$\dot{E}_P$ (kW)	$\dot{E}_L$ (kW)	cost($/h)	C_f ($/GJ)	C_p ($/GJ)	C_D ($/h)	C_L ($/h)	f (%)
AHE	120.00	385.60	245.80	0.00	4.50	9.35	15.19	4.04	0.00	10.26
SOFC	52.16	1333.0	1269.60	0.00	10.57	6.08	8.37	1.14	0.00	89.20
AB	42.62	544.00	501.30	0.00	1.77	8.37	9.35	1.29	0.00	27.27
HRSG	20.07	79.08	59.01	0.00	2.15	9.35	13.67	0.68	0.00	81.20
FHE	8.07	19.74	11.67	0.00	0.28	9.35	16.02	0.27	0.00	2.92
CS	7.11	8.51	2.83	0.00	0.26	8.51	26.00	0.22	0.00	19.96
GT	5.97	101.30	95.30	0.00	0.73	9.35	11.46	3.41	0.00	72.30
AC	3.01	15.90	12.89	0.00	0.44	8.63	18.19	0.09	0.00	78.89
HPG	2.80	14.66	11.81	15.43	1.24	0.00	0.18	0.00	1.18	100.0
HTHEX	1.49	6.83	5.34	0.00	0.05	1.93	4.48	0.01	0.00	78.85
LPG	1.27	4.98	3.72	0.00	0.01	0.46	1.00	0.00	0.00	70.31
LTHEX	0.59	1.97	1.37	0.00	0.03	0.88	6.71	0.00	0.00	93.47
FC	0.06	0.43	0.37	0.00	0.03	8.63	60.28	0.00	0.00	94.20
Pump HRSG	0.04	0.17	0.12	0.00	0.01	8.63	38.30	0.00	0.00	90.29
Pump	0.00	5.00	5.00	0.00	0.01	0.16	10.12	0.00	0.00	100.0
Ro Unit	0.0107	0.0213	0.00523	0.00	20.4	8.42	14.58	6.53	0.00	73.2
Freshwater production rate:256 kg/day										

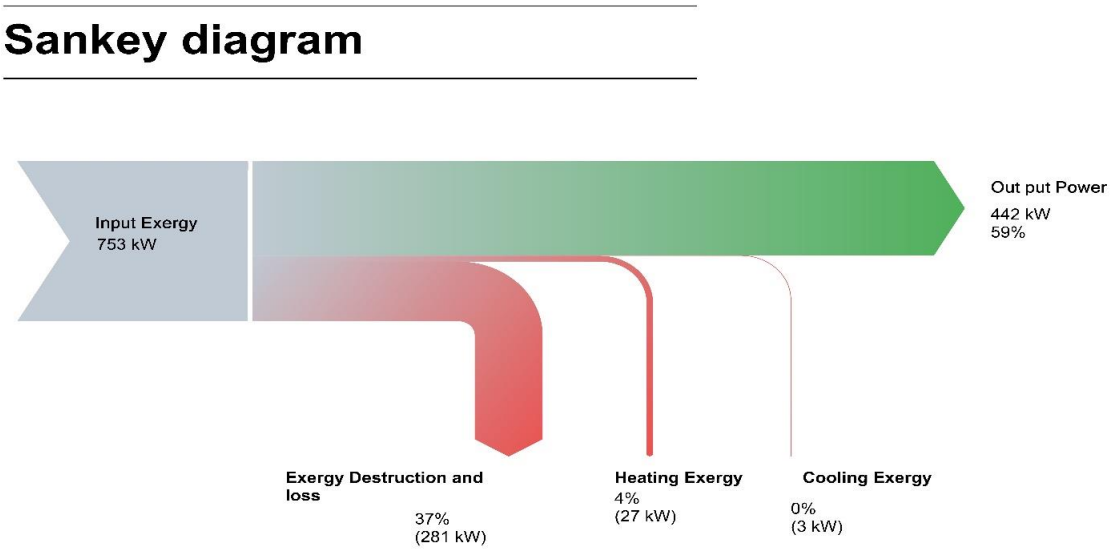

Fig. 7. Sankey diagram for the proposed Energy system

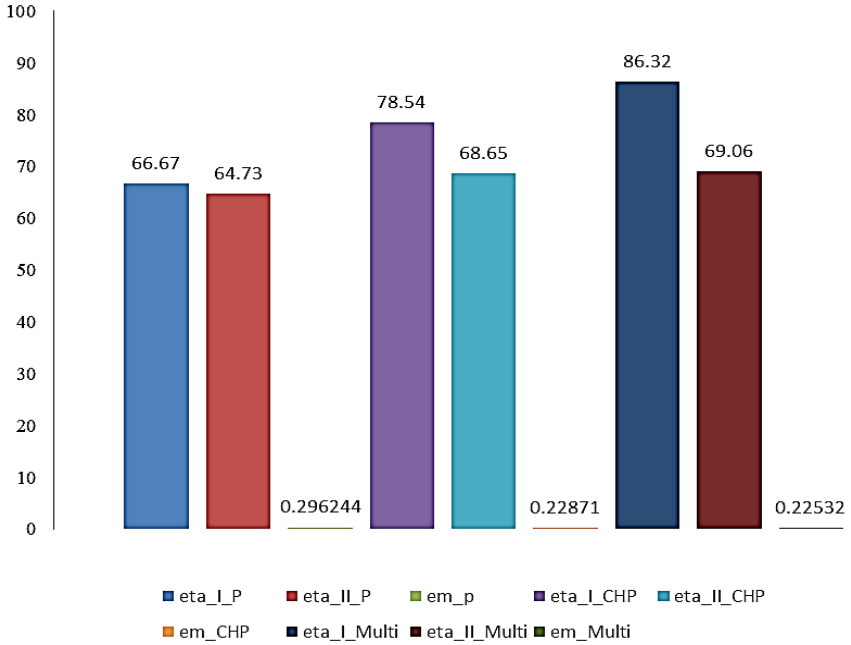

Fig.8 performance indicators of the proposed energy system

5.Conclusion

In this research paper, a multigenerational energy system in a residential scale is proposed and analyzed from energy, exergy, economic, and environmental standpoints. The proposed system has proved to be a promising system to be integrated with buildings since it generates power using hybrid SOFC/GT, heating by the help of an HRSG, cooling utilization, an absorption chiller, and freshwater production utilizing an RO system. The system is put under a parametric study, and the stack temperature difference, fuel utilization factor, current density, and fuel compressor pressure ratio are found to be the most effective parameters in the system performance. Other main verdicts of the current study, as well as parametric study results, ar multi folded as:

- The results of the environmental analysis show an excellent motivation for using integrated systems since it reduces 31% of the GHG emission compared to the standalone power generation system.
- Exergetic efficiency for overall system is 25.73% greater than CHP system and 33.35% greater than single power generation system.
- AHE, SOFC, and AB have the highest values of exergy destruction since they possess three primary sources of irreversibility, which is a chemical reaction, mixing, and high temperature difference.
- The parametric study shows that for specific values of fuel utilization factor, the efficiency increases, and unit product cost decreases, which is of great importance to optimization purposes.
- The system can produce 256 kg/day freshwater, and the total unit product cost of the system is equal to 37.78 ($/GJ).

Acknowledgment

The Authors would like to express the highest gratitude toward members of the Center of excellence in design and optimization at the University of Tehran. Special thanks go to the Tehran Chamber of Commerce Industries Mines and Agriculture, which have covered part of the expenses needed to carry out this research.

References

[1] Behzadi A, Gholamian E, Houshfar E, Ashjaee M, Habibollahzade A. Thermoeconomic analysis of a hybrid PVT solar system integrated with double

effect absorption chiller for cooling/hydrogen production. Energy Equip Syst 2018; 6:41327. https://doi.org/10.22059/ees.2018.33319.

[2] Habibollahzade A, Houshfar E, Ashjaee M, Gholamian E, Behzadi A. Enhanced performance and reduced payback period of a low grade geothermal-based ORC through employing two TEGs. Energy Equip Syst 2019;7:23–39. https://doi.org/10.22059/EES.2019.3461.

[3] Mirzaee M, Zare R, Sadeghzadeh M, Maddah H, Ahmadi MH, Acıkkalp E, et al. Thermodynamic analyses of different scenarios in a CCHP system with micro turbine – Absorption chiller, and heat exchanger. Energy Convers Manag 2019;198:111919. https://doi.org/10.1016/J.ENCONMAN.2019.111919.

[4] Mortazavi Beni H, Ahmadi Nadooshan A, Bayareh M. The energy and exergy analysis of a novel cogeneration organic Rankine power and two-stage compression refrigeration cycle. Energy Equip Syst 2017;5:299–312. https://doi.org/10.22059/ees.2017.27570.

[5] Habibollahzade A, Gholamian E, Houshfar E, Behzadi A. Multi-objective Optimization of Biomass-based Solid Oxide Fuel Cell Integrated with Stirling Engine and Electrolyzer. Energy Convers Manag 2018;171:1116–33. https://doi.org/10.1016/j.enconman.2018.06.061.

[6] Behbahani-nia A, Shams S. Thermoeconomic optimization and exergy analysis of transcritical CO2 refrigeration cycle with an ejector. Energy Equip Syst 2016;4:4352. https://doi.org/10.22059/EES.2016.2016.

[7] Naserian MM, Farahat S, Sarhaddi F. Exergoeconomic analysis and genetic algorithm power optimization of an irreversible regenerative Brayton cycle. Exergoeconomic Anal Genet Algorithm Power Optim an Irreversible Regen Brayt Cycle 2016;4:188–203. https://doi.org/10.22059/ees.2016.59554.

[8] Behzadi A, Gholamian E, Houshfar E, Habibollahzade A. Multi-objective optimization and exergoeconomic analysis of waste heat recovery from Tehran's waste-to-energy plant integrated with an ORC unit. Energy 2018;160:1055–68. https://doi.org/10.1016/J.ENERGY.2018.07.074.

[9] Abbasi M, Chahartaghi M, Hashemian SM. Energy, exergy, and economic evaluations of a CCHP system by using the internal combustion engines and gas turbine as prime movers. Energy Convers Manag 2018;173:359–74. https://doi.org/10.1016/J.ENCONMAN.2018.07.095.

[10] Li M, Mu H, Li N, Ma B. Optimal design and operation strategy for integrated evaluation of CCHP (combined cooling heating and power) system. Energy 2016;99:202–20. https://doi.org/10.1016/J.ENERGY.2016.01.060.

[11] Rajamand S, Ketabi A, Zahedi A. Simultaneous power sharing and protection against faults for DGs in microgrid with different loads. Energy Equip Syst 2019;7:279–95. https://doi.org/10.22059/EES.2019.36564.

[12] Khademi M, Behzadi Forough A, Khosravi A. Techno-economic operation optimization of a HRSG in combined cycle power plants based on evolutionary algorithms: A case study of Yazd, Iran. Energy Equip Syst 2019;7:67–79. https://doi.org/10.22059/EES.2019.34618.

[13] Ghasemkhani A, Farahat S, Naserian MM. The development and assessment of solar-driven Tri-generation system energy and optimization of criteria comparison. Energy Equip Syst 2018;6:367–79. https://doi.org/10.22059/ees.2018.33309.

[14] Mehrpooya M, Sadeghzadeh M, Rahimi A, Pouriman M. Technical performance analysis of a combined cooling heating and power (CCHP) system based on solid oxide fuel cell (SOFC) technology – A building application. Energy Convers Manag 2019;198:111767.

https://doi.org/10.1016/J.ENCONMAN.2019.06.078.

[15] Wang Z, Han W, Zhang N, Liu M, Jin H. Proposal and assessment of a new CCHP system integrating gas turbine and heat-driven cooling/power cogeneration. Energy Convers Manag 2017;144:1–9. https://doi.org/10.1016/J.ENCONMAN.2017.04.043.

[16] Li L, Mu H, Gao W, Li M. Optimization and analysis of CCHP system based on energy loads coupling of residential and office buildings. Appl Energy 2014;136:206–16. https://doi.org/10.1016/J.APENERGY.2014.09.020.

[17] Jing R, Wang M, Brandon N, Zhao Y. Multi-criteria evaluation of solid oxide fuel cell based combined cooling heating and power (SOFC-CCHP) applications for public buildings in China. Energy 2017;141:273–89. https://doi.org/10.1016/J.ENERGY.2017.08.111.

[18] Hossein Abbasi M, Sayyaadi H, Tahmasbzadebaie M. A methodology to obtain the foremost type and optimal size of the prime mover of a CCHP system for a large-scale residential application. Appl Therm Eng 2018;135:389–405. https://doi.org/10.1016/J.APPLTHERMALENG.2018.02.062.

[19] Feng L, Dai X, Mo J, Shi L. Performance assessment of CCHP systems with different cooling supply modes and operation strategies. Energy Convers Manag 2019;192:188–201. https://doi.org/10.1016/J.ENCONMAN.2019.04.048.

[20] Moghimi M, Emadi M, Ahmadi P, Moghadasi H. 4E analysis and multi-objective optimization of a CCHP cycle based on gas turbine and ejector refrigeration. Appl Therm Eng 2018;141:516–30. https://doi.org/10.1016/J.APPLTHERMALENG.2018.05.075.

[21] Al Moussawi H, Fardoun F, Louahlia H. 4-E based optimal management of a SOFC-CCHP system model for residential applications. Energy Convers Manag 2017;151:607–29. https://doi.org/10.1016/J.ENCONMAN.2017.09.020.

[22] Luo XJ, Fong KF. Development of multi-supply-multi-demand control strategy for combined cooling, heating and power system primed with solid oxide fuel cell-gas turbine. Energy Convers Manag 2017;154:538–61. https://doi.org/10.1016/J.ENCONMAN.2017.11.032.

[23] Chen X, Zhou H, Li W, Yu Z, Gong G, Yan Y, et al. Multi-criteria assessment and optimization study on 5 kW PEMFC based residential CCHP system. Energy Convers Manag 2018;160:384–95. https://doi.org/10.1016/J.ENCONMAN.2018.01.050.

[24] Chitgar N, Emadi MA, Chitsaz A, Rosen MA. Investigation of a novel multigeneration system driven by a SOFC for electricity and fresh water production. Energy Convers Manag 2019;196:296–310. https://doi.org/10.1016/J.ENCONMAN.2019.06.006.

[25] Behzadi A, Gholamian E, Ahmadi P, Habibollahzade A, Ashjaee M. Energy, exergy and exergoeconomic (3E) analyses and multi-objective optimization of a solar and geothermal based integrated energy system. Appl Therm Eng 2018;143:1011–22. https://doi.org/10.1016/J.APPLTHERMALENG.2018.08.034.

[26] Gholamian E, Zare V, Mousavi SM. Integration of biomass gasification with a solid oxide fuel cell in a combined cooling, heating and power system: A thermodynamic and environmental analysis. Int J Hydrogen Energy 2016. https://doi.org/10.1016/j.ijhydene.2016.07.217.

[27] Behzadi A, Habibollahzade A, Zare V, Ashjaee M. Multi-objective optimization of a hybrid biomass-based SOFC/GT/double effect absorption chiller/RO desalination system with CO2 recycle. Energy Convers Manag 2019;181:302–18. https://doi.org/10.1016/J.ENCONMAN.2018.11.053.

[28] Bejan A, Tsatsaronis G. Thermal design and optimization. John Wiley & Sons; 1996.

[29] Ahmadi P, Dincer I, Rosen MA. Multi-objective optimization of a novel solar-based multigeneration energy system. Sol Energy 2014;108:576–91. https://doi.org/10.1016/j.solener.2014.07.022.

[30] Gholamian E, Zare V. A comparative thermodynamic investigation with environmental analysis of SOFC waste heat to power conversion employing Kalina and Organic Rankine Cycles. Energy Convers Manag 2016;117. https://doi.org/10.1016/j.enconman.2016.03.011.

[31] Yari M, Mehr AS, Mahmoudi SMS, Santarelli M. A comparative study of two SOFC based cogeneration systems fed by municipal solid waste by means of either the gasifier or digester. Energy 2016;114:586–602. https://doi.org/10.1016/j.energy.2016.08.035.

[32] Gholamian E, Hanafizadeh P, Ahmadi P, Mazzarella L. 4E analysis and three-objective optimization for selection of the best prime mover in smart energy systems for residential applications: a comparison of four different scenarios. J Therm Anal Calorim 2020. https://doi.org/10.1007/s10973-020-10177-0.

[33] Khani L, Mehr AS, Yari M, Mahmoudi SMS. Multi-objective optimization of an indirectly integrated solid oxide fuel cell-gas turbine cogeneration system. Int J Hydrogen Energy 2016;41:21470–88. https://doi.org/10.1016/J.IJHYDENE.2016.09.023.

[34] Dincer I, Rosen MA, Ahmadi P. Optimization of Energy Systems. John Wiley & Sons,; 2017.

[35] Behzadi A, Arabkoohsar A, Gholamian E. Multi-criteria optimization of a biomass-fired proton exchange membrane fuel cell integrated with organic rankine cycle/thermoelectric generator using different gasification agents. Energy 2020;201:117640. https://doi.org/10.1016/J.ENERGY.2020.117640.

[36] Gholamian E, Hanafizadeh P, Ahmadi P, Mazzarella L. A transient optimization and techno-economic assessment of a building integrated combined cooling, heating and power system in Tehran. Energy Convers Manag 2020;217:112962. https://doi.org/10.1016/J.ENCONMAN.2020.112962.

[37] Bejan A, Moran MJ. Thermal design and optimization. John Wiley & Sons; 1996.

[38] Wu C, Wang S sen, Feng X jia, Li J. Energy, exergy and exergoeconomic analyses of a combined supercritical CO2 recompression Brayton/absorption refrigeration cycle. Energy Convers Manag 2017;148:360–77. https://doi.org/10.1016/j.enconman.2017.05.042.

[39] Balli O, Aras H, Hepbasli A. Thermodynamic and thermoeconomic analyses of a trigeneration (TRIGEN) system with a gas-diesel engine: Part I - Methodology. Energy Convers Manag 2010;51:2252–9. https://doi.org/10.1016/j.enconman.2010.03.021.

[40] Indicators E. Marshall&Swift Equipment Cost Index. Chem Eng 2011:72.

[41] Dinçer I, Rosen M, Ahmadi P. Optimization of energy systems. John Wiley & Sons; 2017.

[42] Rokni M. Thermodynamic and thermoeconomic analysis of a system with biomass gasification, solid oxide fuel cell (SOFC) and Stirling engine. Energy 2014;76:19–31. https://doi.org/10.1016/j.energy.2014.01.106.

[43] Sánchez D, Chacartegui R, Torres M, Sánchez T. Stirling based fuel cell hybrid systems : An alternative for molten carbonate fuel cells 2009;192:84–93. https://doi.org/10.1016/j.jpowsour.2008.12.061.

[44] Assar M, Blumberg T, Morosuk T, Tsatsaronis G. Comparative exergoeconomic evaluation of two

modern combined-cycle power plants. Energy Convers Manag 2016;153:616–26. https://doi.org/10.1016/j.enconman.2017.10.036.

[45] Landau L, Moran MJ, Shapiro HN, Boettner DD, Bailey M. Fundamentals of engineering thermodynamics. John Wiley & Sons; 2010.

[46] Bejan A, Tsatsaronis G (George), Moran MJ. Thermal design and optimization. Wiley; 1996.

[47] Gholamian E, Hanafizadeh P, Ahmadi P. Advanced exergy analysis of a carbon dioxide ammonia cascade refrigeration system. Appl Therm Eng 2018;137. https://doi.org/10.1016/j.applthermaleng.2018.03.055.

[48] Yari M, Mehr AS, Mahmoudi SMS, Santarelli M. A comparative study of two SOFC based cogeneration systems fed by municipal solid waste by means of either the gasifier or digester. Energy 2016;114:586–602. https://doi.org/10.1016/j.energy.2016.08.035.

[49] Ahmadi P, Dincer I, Rosen MA. Exergy, exergoeconomic and environmental analyses and evolutionary algorithm based multi-objective optimization of combined cycle power plants. Energy 2011;36:5886–98. https://doi.org/10.1016/J.ENERGY.2011.08.034.

[50] Gholamian E, Hanafizadeh P, Ahmadi P. Exergo-economic analysis of a hybrid anode and cathode recycling SOFC/Stirling engine for aviation applications. Int J Sustain Aviat 2018; 4:11. https://doi.org/10.1504/IJSA.2018.09295

[51] Tao G, Armstrong T, Virkar A. Intermediate temperature solid oxide fuel cell (IT-SOFC) research and development activities at MSRI. Ninet. Annu. ACERC&ICES Conf. Utah, 2005.

[52] Nemati A, Sadeghi M, Yari M. Exergoeconomic analysis and multi-objective optimization of a marine engine waste heat driven RO desalination system integrated with an organic Rankine cycle using zeotropic working fl uid. Desalination 2017;422:113–23. https://doi.org/10.1016/j.desal.2017.08.012.

[53] Gomri R, Hakimi R. Second law analysis of double effect vapour absorption cooler system. Energy Convers Manag 2008; 49:3343–8.